

Gradient enhanced damage: modelling, implementation and applications

Anton Matzenmiller^{1,2}, Henning Schmidt^{1,3}, Marvin Nahrman¹

¹Institute of Mechanics, Department of Mechanical Engineering, University of Kassel,
Mönchebergstr. 7, 34125 Kassel, Germany

²Professor of Applied Mechanics

³Bertrandt Simulations GmbH

Abstract

Finite element (FE) simulations with constitutive models for softening materials, such as in the case of standard continuum damage mechanics based approaches, suffer from pathological mesh sensitivity as a result of strain localisation into a single element row. To overcome this major drawback, the local damage has to be enhanced towards nonlocal damage evolution. A suitable method for this purpose is the integral nonlocal formulation, available in LS-DYNA® by the keyword ***MAT_NONLOCAL**. However, its costly underlying search algorithm can result in a strong increase of the simulation time, leading to an impractical application for engineering problems.

This paper presents the modelling and implementation of a gradient enhanced nonlocal damage model, based on a TAYLOR series expansion of the integral nonlocal formulation. The resulting HELMHOLTZ type differential equation represents an analogous field problem to the heat equation, allowing a very efficient implementation into LS-DYNA® by exploiting its thermo-mechanical coupled solver. Thereby, the nodal temperature is replaced by the nonlocal damage variable. The implementation is discussed in detail and verified by means of a simple tensile bar simulation.

The gradient enhanced damage model is applied to two existing continuum damage models, demonstrating the versatile range of application and the simplicity of integrating the gradient enhancement for user defined material models. Therefore, a stress state dependent damage approach for ductile steels is considered as well as a failure model for hyperelastic polyurethane (PUR) based adhesives. The simulation results are compared to the according test data for various specimens, showing a good agreement within the region of softening material behaviour. Moreover, mesh insensitivity is demonstrated and a critical comparison with the ***MAT_NONLOCAL** model is carried out, revealing a strong reduction of the simulation time in favour of the gradient enhanced damage method instead of the ***MAT_NONLOCAL** option.

Keywords

gradient enhanced damage, nonlocal damage, user implementation, ductile steel, PUR adhesive

1 Introduction and motivation

Material softening is characterised by a stress decrease for progressing strains. This inherently provokes material instability, because DRUCKER's stability criterion [1] is violated. The consequence is the onset of strain localisation. Thereby, the complete deformation occurs within a narrow region of the structure, denoted as *localisation zone*, whereas elastic unloading arises outside of it. However, finite element simulations with softening material models lead to a localisation of the strains into a single element row. As a result, the localisation zone is meshsize dependent and converges towards zero length with mesh refinement.

The localisation phenomenon is demonstrated in depth by the numerical analysis of a three-dimensional bar under uniaxial tension, whereby a coupled plasticity-damage model is applied for the material behaviour. The parameters of linear elasticity are $E=210000$ MPa and $\nu=0.3$. The yield stress $\kappa_0=400$ MPa and the isotropic hardening modulus $E_\kappa=1000$ MPa are determined for the plasticity model. The linear damage evolution according to [2] is initiated, when the equivalent plastic strain reaches the critical strain parameter $\varepsilon_c=0.05$ and failure is obtained for $\varepsilon_f=0.2$.

The FE model is depicted in Fig. 1 with its geometric dimensions. The boundary conditions are chosen to provide a uniaxial state of tensile stress. Therefore, the nodal displacements of the fixed end are constrained in the z -direction and the axial nodal displacements of the free end are prescribed by the function

$$u(t) = L_0 [\exp(\dot{\varepsilon}_{\log} t) - 1], \quad (1)$$

whereby the logarithmic strain rate $\dot{\varepsilon}_{\log}=1.0$ s⁻¹ is constant. The discretisation of the bar is carried out equidistantly with 8, 16, 32 and 64 elements in axial direction, entailing equal element lengths. The cross-section area of each element is 1 mm². In order to trigger localisation in the first element at the fixed end, the initial yield stress of this weakened element is decreased by 0.01 %.

The simulation results are depicted in Fig. 2. Here, the strong mesh sensitivity of the predicted stress-strain curves is pointed out. Consequently, the dissipated energy due to softening depends highly on the number of elements and converges towards zero with mesh refinement. Moreover, the damage variable is localised in nearly one single element leading to a mesh size dependent damage zone.

To overcome these issues, softening material models have to be extended by a suitable regularisation

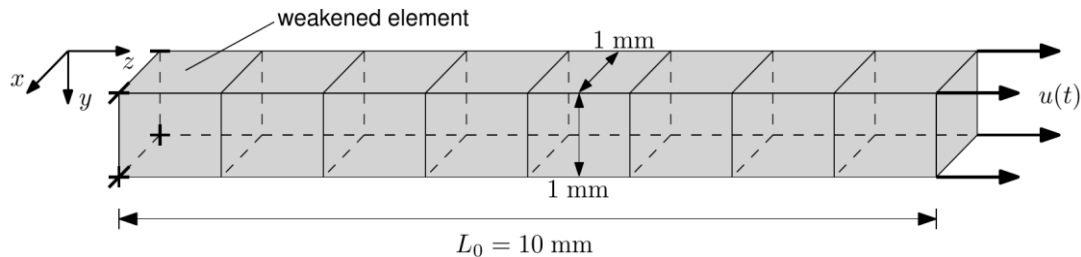


Fig. 1: FE model of three-dimensional bar with geometric dimensions and boundary conditions

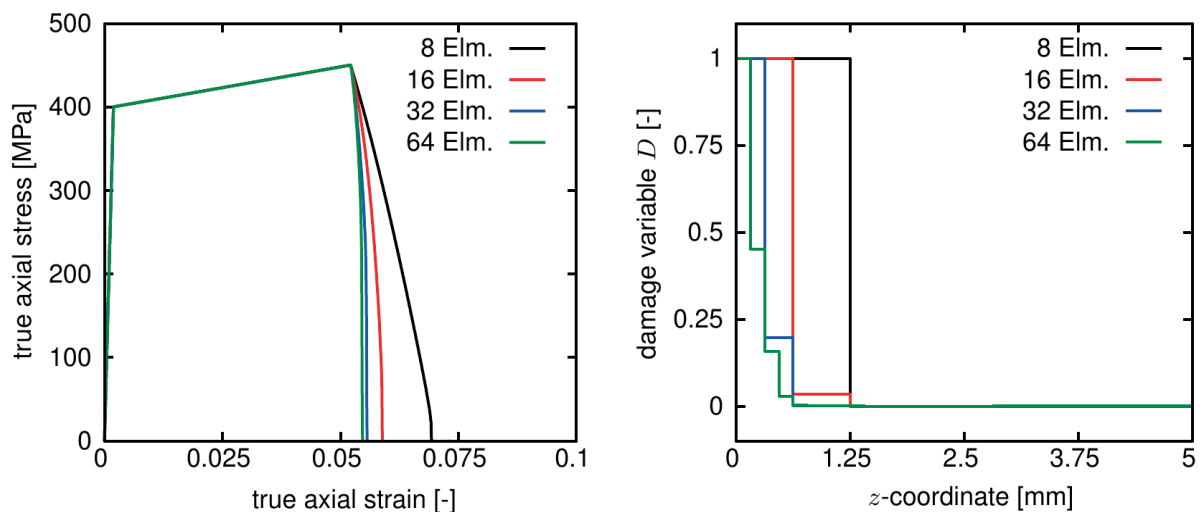


Fig. 2: True axial stress-strain curves (left) and damage variable prior to failure along the z -coordinate (right) for 8, 16, 32 and 64 elements

method. Besides element size dependent failure parameters, the viscous regularisation, the integral nonlocal formulation and the gradient enhanced damage approach are in the focus of recent research activities, see [3], [4] and [5]. However, the implementation into LS-DYNA® is still missing. Therefore, this contribution closes this gap by presenting the modelling approach and the implementation of the gradient enhanced nonlocal damage model into LS-DYNA® on the basis of user interfaces for material models.

2 Theory of gradient enhanced damage

The gradient enhanced damage approach is based on the approximation of the integral nonlocal formulation, which is proposed in [6]. Here, the arbitrary local field variable $z(\mathbf{y})$ at the neighbouring points \mathbf{y} is weighted over a certain integration region Ω by means of the weighting function $w(\mathbf{x}, \mathbf{y})$. This leads to the nonlocal field variable $\tilde{z}(\mathbf{x})$ at the reference point \mathbf{x} .

$$\tilde{z}(\mathbf{x}) = \frac{1}{W(\mathbf{x})} \int_{\Omega} z(\mathbf{y}) w(\mathbf{x}, \mathbf{y}) d\mathbf{y}, \quad W(\mathbf{x}) = \int_{\Omega} w(\mathbf{x}, \mathbf{y}) d\mathbf{y} \quad (2)$$

The integration region is determined by the characteristic length l_c , which has to be larger than the element length, ensuring a successful regularisation. In order to provide a bell-curved distribution of the field variable, the three-parameter function

$$w(\mathbf{x}, \mathbf{y}) = \left[1 + \left(\frac{\|\mathbf{x} - \mathbf{y}\|}{l_c} \right)^p \right]^{-q} \quad (3)$$

is applied, containing the two parameters p and q for the shape specification in addition to the length parameter l_c . Thereby, the parameter p controls the size of the damage zone and q influences the smoothness of the decline. Note that the weighting function is only valid within the integration region. The nonlocal integral approach is already available in LS-DYNA® by means of the keyword ***MAT_NONLOCAL**, see the LS-DYNA® manual [7]. Here, the three-parameter weighting function is inbuilt and not replaceable. The ***MAT_NONLOCAL** option can be applied to an arbitrary local variable for the nonlocal algorithm, whereby it is possible to employ several variables simultaneously for the regularisation.

Gradient enhanced damage models are based on the approximation of the integral nonlocal formulation by means of a TAYLOR series expansion and are applicable for arbitrary local scalar field variables $z(\mathbf{x})$. The TAYLOR series is developed about the reference point \mathbf{x} and approximates $z(\mathbf{y})$ at the neighbouring point \mathbf{y} by:

$$z(\mathbf{y}) = z(\mathbf{x}) + \nabla z(\mathbf{x}) \cdot (\mathbf{x} - \mathbf{y}) + \frac{1}{2!} \nabla^2 z(\mathbf{x}) \cdot^2 (\mathbf{x} - \mathbf{y})^2 + \frac{1}{3!} \nabla^3 z(\mathbf{x}) \cdot^3 (\mathbf{x} - \mathbf{y})^3 + \frac{1}{4!} \nabla^4 z(\mathbf{x}) \cdot^4 (\mathbf{x} - \mathbf{y})^4 + \frac{1}{5!} \nabla^5 z(\mathbf{x}) \cdot^5 (\mathbf{x} - \mathbf{y})^5 + \frac{1}{6!} \nabla^6 z(\mathbf{x}) \cdot^6 (\mathbf{x} - \mathbf{y})^6 + \dots \quad (4)$$

Here, ∇^n is the n -th order gradient operator, \cdot^n is the n -th order inner product, and $(\mathbf{x} - \mathbf{y})^n$ the n -factor dyadic product of the distance $(\mathbf{x} - \mathbf{y})$, see also p. 3392 f. of [8].

Inserting Eq. (4) into the integral nonlocal approach, Eq. (2) leads to the nonlocal field variable

$$\tilde{z}(\mathbf{x}) = z(\mathbf{x}) + c_1 \nabla^2 z(\mathbf{x}) + c_2 \nabla^4 z(\mathbf{x}) + c_3 \nabla^6 z(\mathbf{x}) + \dots \quad (5)$$

Here, the odd terms are neglected, since the weighting function Eq. (3) is symmetric, see also p. 3393 f. of [8]. Then, Eq. (5) is rearranged towards the local field variable $z(\mathbf{x})$ and the second-order gradient ∇^2 is applied:

$$\nabla^2 z(\mathbf{x}) = \nabla^2 \tilde{z}(\mathbf{x}) - c_1 \nabla^4 z(\mathbf{x}) - c_2 \nabla^6 z(\mathbf{x}) - c_3 \nabla^8 z(\mathbf{x}) - \dots \quad (6)$$

The next step is the insertion of Eq. (6) into Eq. (5):

$$\tilde{z}(\mathbf{x}) = z(\mathbf{x}) + c_1 (\nabla^2 \tilde{z}(\mathbf{x}) - c_1 \nabla^4 z(\mathbf{x}) - c_2 \nabla^6 z(\mathbf{x}) - c_3 \nabla^8 z(\mathbf{x}) - \dots) + c_2 \nabla^4 z(\mathbf{x}) + c_3 \nabla^6 z(\mathbf{x}) + \dots \quad (7)$$

The factorisation with respect to the gradients leads to:

$$\tilde{z}(\mathbf{x}) = z(\mathbf{x}) + c_1 \nabla^2 \tilde{z}(\mathbf{x}) + (c_2 - c_1^2) \nabla^4 z(\mathbf{x}) + (c_3 - c_1 c_2) \nabla^6 z(\mathbf{x}) + \dots \quad (8)$$

Finally, the nonlocal field variable $\tilde{z}(\mathbf{x})$ is separated from the local one $z(\mathbf{x})$:

$$\tilde{z}(\mathbf{x}) - c_1 \nabla^2 \tilde{z}(\mathbf{x}) = z(\mathbf{x}) + (c_2 - c_1^2) \nabla^4 z(\mathbf{x}) + (c_3 - c_1 c_2) \nabla^6 z(\mathbf{x}) + \dots \quad (9)$$

Only the second-order term is applied within the TAYLOR series and the higher-order terms are neglected. The parameter c_1 is replaced by the characteristic length l_c^2 , resulting in

$$\tilde{z}(\mathbf{x}) - l_c^2 \nabla^2 \tilde{z}(\mathbf{x}) = z(\mathbf{x}) \quad (10)$$

Due to its implicit nature, this approach is denoted as implicit second-order gradient approximation, see also p. 131 of [9] and p. 3393 of [8]. Moreover, Eq. (10) is a HELMHOLTZ type inhomogeneous differential equation. For $l_c \rightarrow 0$, the local formulation is obtained. In the following, the framework of the implicit gradient enhancement is applied to the local damage variable $D(\mathbf{x})$ as the right hand side for the determination of the unknown nonlocal damage $\tilde{D}(\mathbf{x})$:

$$\tilde{D}(\mathbf{x}) - l_c^2 \nabla^2 \tilde{D}(\mathbf{x}) = D(\mathbf{x}) \quad (11)$$

3 Efficient implementation based on user interfaces

An analogous field problem of the gradient enhanced nonlocal damage model, based on Eq. (11), is used to implement this model in an efficient manner. The stationary heat conduction equation with a temperature dependent heat source $r(T(\mathbf{x}))$ is given by

$$k \nabla^2 T(\mathbf{x}) = -r(T(\mathbf{x})) \quad (12)$$

with k as the heat conduction parameter and $T(\mathbf{x})$ as the temperature at point \mathbf{x} . The stationary heat conduction equation in this form is a differential equation of the same kind as Eq. (11). By comparing Eq. (12) to Eq. (11) in the following homogeneous form

$$k \nabla^2 T(\mathbf{x}) + r(T(\mathbf{x})) = 0 \quad \rightarrow \quad l_c^2 \nabla^2 \tilde{D}(\mathbf{x}) - \tilde{D}(\mathbf{x}) + D(\mathbf{x}) = 0, \quad (13)$$

the heat source term $r(T(\mathbf{x}))$ provides the necessary substitutions among others in Tab. 1.

Table 1: Substitution for the analogous field problem between gradient nonlocal model Eq. (11) and the stationary heat equation Eq. (12)

Stationary heat conduction equation	Gradient enhanced nonlocal damage
k	l_c^2
$T(\mathbf{x})$	$\tilde{D}(\mathbf{x})$
$r(T(\mathbf{x}))$	$-\tilde{D}(\mathbf{x}) + D(\mathbf{x})$

By solving the heat equation (12) and applying the substitutions in Tab. 1, the nonlocal damage $\tilde{D}(\mathbf{x})$ is calculated instead of the temperature $T(\mathbf{x})$. The thermal solver provided by LS-DYNA® is able to solve heat conduction problems with a temperature dependent source term. With this capability, the implementation of the gradient enhanced nonlocal damage model reduces to applying the right substitution in order to let the thermal solver calculate the nonlocal damage and, thus, regularise the local damage variable.

In LS-DYNA®, each property can be assigned to a mechanical and a thermal boundary value problem. In this contribution, the implementation of the gradient enhanced regularisation model relies on the possibility of bidirectional communication between the thermal and mechanical model. Fig. 4 shows the flow chart of the implementation of the gradient enhanced damage model using LS-DYNA®. In the following, the adaptation in the user subroutines to the thermal and the mechanical boundary value problem is discussed.

User defined thermal material model

The user defined thermal material model can be implemented in one of the `thumat` subroutines, which can be found in the `dyn21.f` file.

The thermal material model provides the necessary substitution so that the thermal solver calculates the nonlocal damage variable instead of the temperature. In LS-DYNA®, the variables in Tab. 2 are used for the implementation of the regularisation model.

Table 2: Substitution for the implementation of the gradient enhanced damage model using the thermal solver provided by LS-DYNA®

Thermal equation	Variable in <code>thumat</code>	Nonlocal variable	Nonlocal damage Eq.
Heat conduction	C1	l_c^2	Nonlocal length squared
Heat source	hsrcl	$-\tilde{D}(x) + D(x)$	Nonlocal minus local damage
Heat source derivative with respect to T	dhsrcldtl	-1	Derivative with respect to $\tilde{D}(x)$
Switch to activate the heat source term	ihsrcl	1	-

The user specifies the nonlocal length in the thermal material card. This value determines how strong the regularisation smooths the damage localisation. The nonlocal length is squared and written into the heat conduction parameter “C1”. For the substitution of the heat source, it is necessary to have a bidirectional communication between the mechanical and the thermal part.

The local damage D is calculated in the mechanical material routine and stored as history variable $hsv(n)$. It is saved in the thermal model in $hsvm(7+n)$. The entries 1 to 7 in $hsvm$ are reserved for the effective stress tensor and the effective plastic strain. The other summand of the heat source $-\tilde{D}$ is the nonlocal damage. By following the substitutions in Tab. 1, the nonlocal damage is equivalent to the temperature in the stationary heat equation. This leads to the expression:

$$hsrcl = -temp + hsvm(7 + n). \quad (14)$$

The derivative of the heat source with respect to T is needed, because the heat source is a function of the temperature and, therefore, the solver demands the derivative of the heat source. For the solution of this boundary value problem LS-DYNA® provides a nonlinear solver provoked by the keyword `*CONTROL_THERMAL_NONLINEAR`. By setting `ihsrcl` to 1, the thermal solver takes the heat source into account.

With the substitutions mentioned above, the thermal solver implemented in LS-DYNA® is now able to calculate the nonlocal damage of the current thermal time step \tilde{D}^{m+1} . The nonlocal damage can then be used in the mechanical material model to calculate the nominal stresses. The time step of the thermal solver is set in the `*CONTROL_THERMAL_TIMESTEP` by the value `IST`. This time step can be chosen at will, but in order to reduce the calculation time of the simulation the thermal time steps Δt^T tends to be much bigger than the mechanical time step Δt^m . As a reference value the thermal time step should be between 100 and 1000 times larger than the mechanical one. LS-DYNA® uses the staggered solution scheme, depicted in Fig. 3, to determine whether to start the thermal or mechanical subroutine.

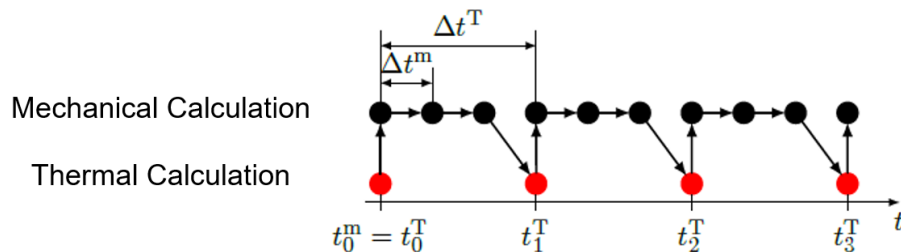


Fig.3: Staggered solution scheme used by LS-DYNA® for thermo-mechanical coupled problems

LS-DYNA® will start the mechanical calculation as long as the time of the next mechanical time step is smaller than the time for the next thermal calculation. The nonlocal damage \tilde{D} will not be calculated as often as the local damage D , because the local damage is calculated in every mechanical time step. This circumstance could be a problem during the calculation, but the time step difference did not prevent the regularisation in the verification and validation examples presented in this contribution. The calculated nonlocal damage value \tilde{D}^{m+1} can now be used in the mechanical material model.

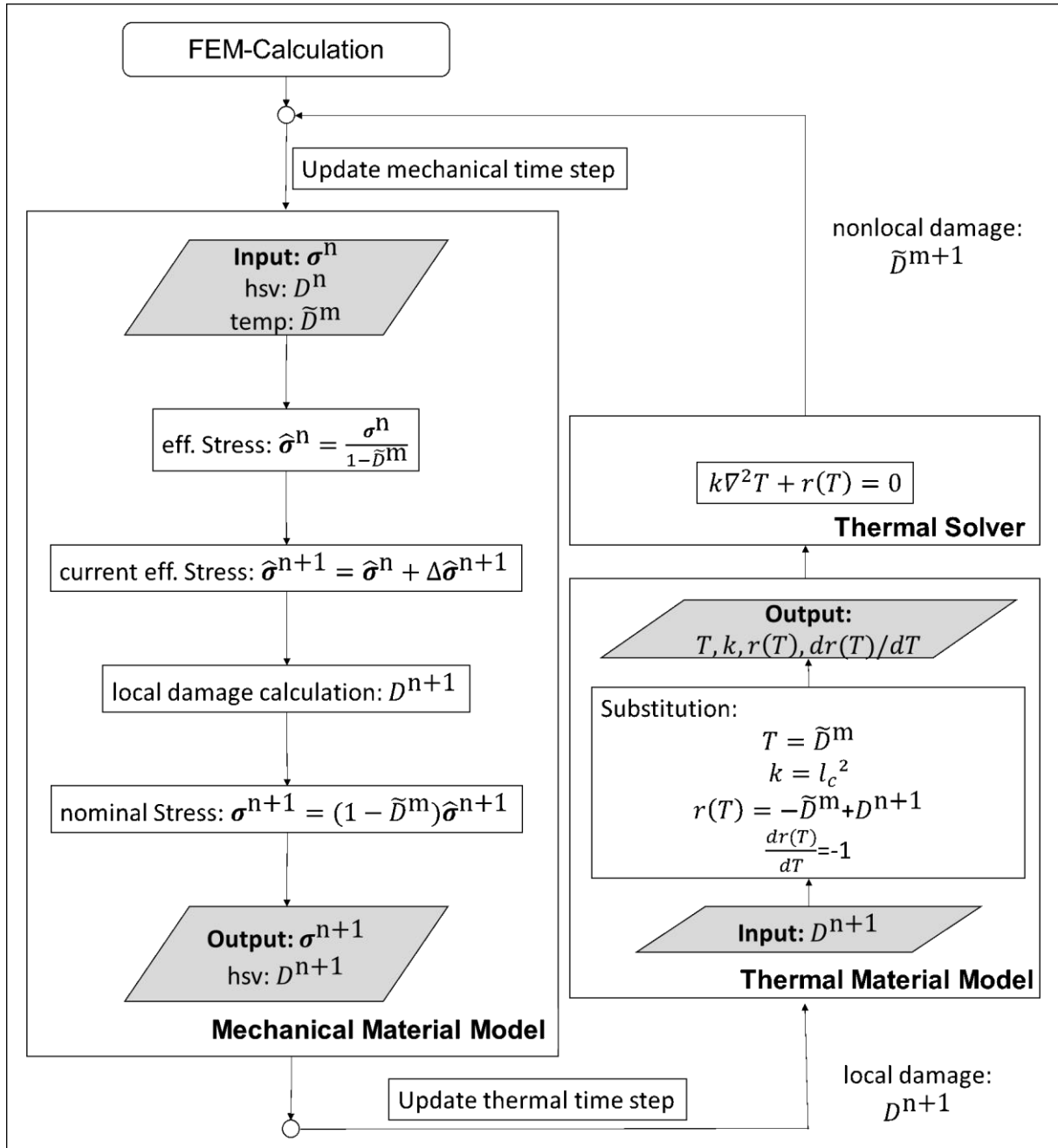


Fig.4: Flowchart of the implementation of the gradient enhanced damage model applying user defined material routines in LS-DYNA®

User defined mechanical material model

The user defined mechanical material model is implemented in one of the `umat` subroutines, which can be found in the `dyn21.f` file. The material model at hand applies the concept of effective stress according to [10] by

$$\hat{\sigma} = \frac{\sigma}{1 - D}, \quad (15)$$

with the effective stress $\hat{\sigma}$, the nominal stress σ and the local damage variable D . A typical procedure of a material model with damage based on the effective stress concept is described in the following.

Starting with the calculation of the effective stress of the previous mechanical time step n

$$\hat{\sigma}^n = \frac{\sigma^n}{1 - \tilde{D}^m} \quad (16)$$

the nonlocal damage \tilde{D}^{m+1} of the current thermal time step $m+1$ is applied for the calculation of the effective stress. The nonlocal damage can be found in the temperature variable *temper*.

The temperature value is available in a mechanical subroutine if the *ITHERM* option in the user defined material card is activated. The local damage is not used in any calculation of the effective or nominal stress, because the regularisation is based on the use of the nonlocal damage variable \tilde{D} . Afterwards, the nominal stress increment of the current time step $\Delta\hat{\sigma}^{n+1}$ is calculated. This procedure depends completely on the material model at hand and the gradient enhanced damage model does not interfere with this calculation. Therefore, it can be easily implemented in a variety of material models, leading to a big advantage of the implementation. Two application examples are shown in chapter 4.

The nominal stress increment of the current time step is added to the nominal stress of the old time step in order to calculate the nominal stress of the current time step:

$$\hat{\sigma}^{n+1} = \hat{\sigma}^n + \Delta\hat{\sigma}^{n+1} \quad (17)$$

The calculation of the current local damage D^{n+1} is again dependent on the material model at hand. This local damage is regularised in the thermal calculation. As shown above, the local damage is calculated in every mechanical time step n and, therefore, generally much more often than the thermal time step m , in which the nonlocal damage \tilde{D} is calculated.

The effective stresses are calculated by using the current nonlocal damage

$$\hat{\sigma}^{n+1} = (1 - \tilde{D}^m) \hat{\sigma}^{n+1}, \quad (18)$$

resulting in a regularised material model as a consequence as well as a reduced mesh dependency during strain softening.

Limitations of the implementation

The implementation of the gradient enhanced damage model is very straight forward, because of the field analogy discussed and the extensive properties of the thermal solver provided by LS-DYNA®. However, there are few limitations due to the efficient implementation. The gradient enhanced damage model can only be applied to isotropic damage models because it regularises only a scalar variable, which is substituted with the temperature. However, the vast majority of damage models are isotropic. Furthermore, it is not possible to use the *IFAIL* option with the implementation of the gradient enhanced damage model in LS-DYNA®. With the *IFAIL* option, elements are deleted as soon as they reach the critical damage value. This method can be used to calculate the fracture path along a damaged area. By using the gradient enhanced damage model, the calculation will run into an *Error Termination* statement as soon as the first element is deleted. Therefore, the *IFAIL* option is not used and the failed elements are stress free but still visible in the d3plot.

4 Verification of the implementation

The implementation of the gradient enhanced damage approach is verified by the numerical analysis of the tensile bar example, presented already in chapter 1. Thereby, the parameter $l_c=1.2$ is applied for the internal length parameter of the gradient enhanced damage approach. The resulting stress-strain curves and the distribution of the nonlocal damage variable prior to failure along the z-direction are shown in Fig. 6. The results are compared to the solution, obtained by the integral nonlocal formulation, with the ***MAT_NONLOCAL** keyword, depicted in Fig. 5. Here, the parameters $p=2$, $q=6$, and $l_c=4$ are chosen for the three-parameter weighting function $w(\mathbf{x}, \mathbf{y})$. For both different nonlocal methods, the results clearly demonstrate the prevention of damage localisation into one single element, whereby the distribution of the damage variable follows a bell-shaped curve. The mesh refinement leads to a converging solution in terms of stress-strain curves, providing non-zero energy dissipation during failure. As a result, the gradient enhanced damage approach leads to a successful regularisation, verifying the implementation into LS-DYNA® by means of the user interfaces. Moreover, both nonlocal options lead to nearly identical results.

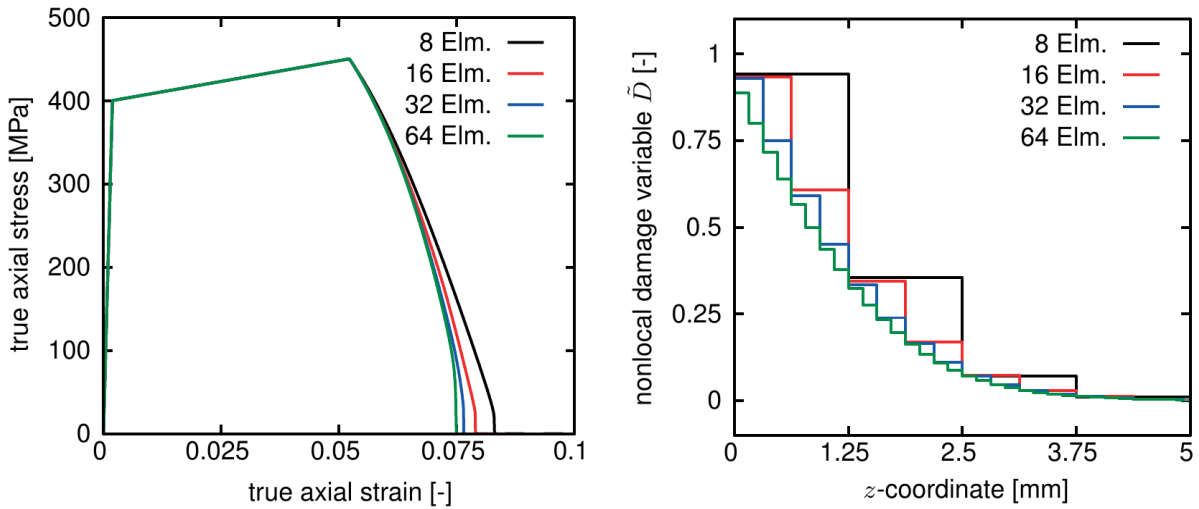


Fig.5: True axial stress-strain curves (left) and nonlocal damage variable prior to failure along the z-coordinate (right) for 8, 16, 32 and 64 elements for the integral nonlocal method

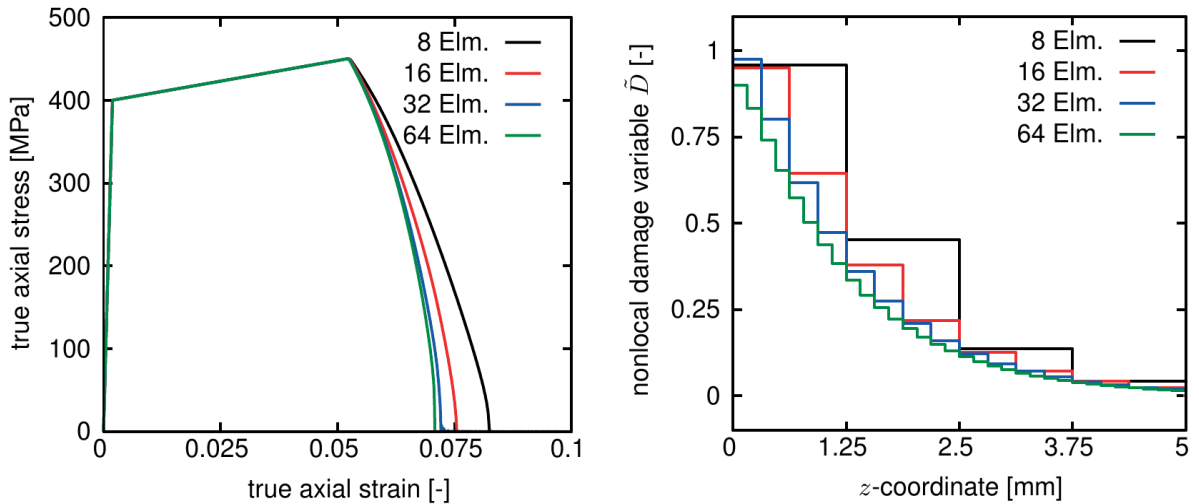


Fig.6: True axial stress-strain curves (left) and nonlocal damage variable prior to failure along the z-coordinate (right) for 8, 16, 32 and 64 elements for the gradient enhanced damage approach

5 Application examples

The implementation of the gradient enhanced damage method is applied to two existing continuum damage models: a stress state dependent damage approach for ductile steels and a failure model for hyperelastic PUR adhesives. Both models are already available as a user defined material model in LS-DYNA® and are enhanced by the gradient enhanced damage approach according to the previous sections.

5.1 Stress state dependent damage approach for ductile steel sheets

A stress state dependent continuum damage model is proposed in [13], [14] and [15] by applying the triaxiality and the LODE parameter dependent critical and failure strain function, according to the HOSFORD-COULOMB model in [16], which is enhanced towards nonlocal damage evolution by employing the integral nonlocal formulation `*MAT_NONLOCAL`. As an alternative, the nonlocal extension is realised by the gradient enhanced damage approach as well. The identified model parameters are already published in [13].

The numerical results are compared to the test data [17] of six different tensile and shear specimens in Fig. 7 a) and b). The sheet thickness is 1.5 mm in all cases. A good overall accordance is achieved, verifying the proposed model for a wide range of stress states. Note that the numerical results, obtained by both different nonlocal methods, are nearly identical. However, a significant difference is found for the elapsed simulation run time. Thereby, three different mesh sizes are evaluated for the smooth tension specimen in Fig. 7 c) and for the 0° shear specimen in d). Compared to the simulation with the gradient enhanced approach, the elapsed simulation time for the integral nonlocal formulation is noticeably higher, in particular for the very fine mesh, due to its underlying costly search algorithm.

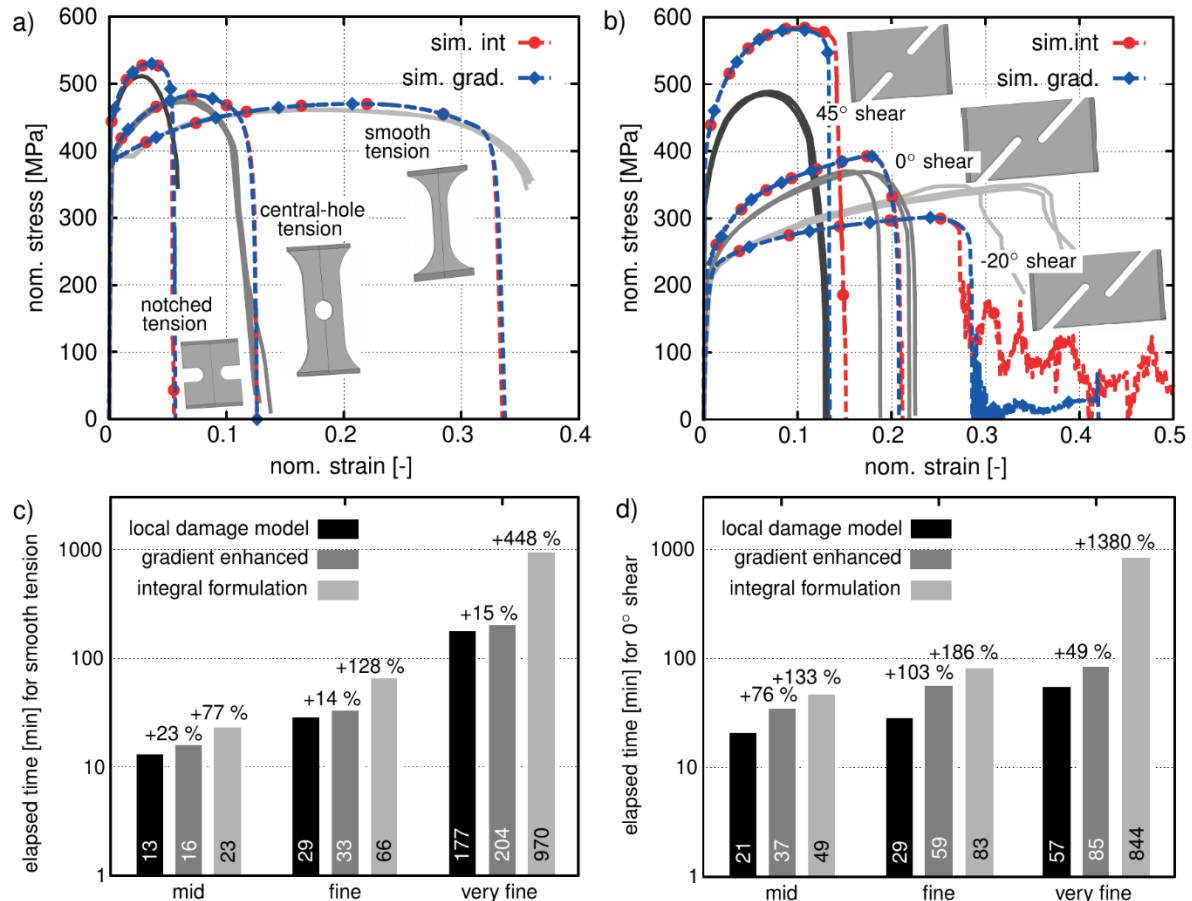


Fig.7: Simulation results by the integral nonlocal model (sim. int.) and the gradient enhanced approach (sim. grad.) compared to test data from [17] (solid lines) for tensile specimens in a) and shear specimens in b) as well as elapsed simulation time for the smooth tension specimen in c) and the 0° shear specimen in d) with three different mesh sizes (mid: 0.5 mm, fine: 0.25 mm, very fine: 0.125 mm), adopted from [15]

5.2 Damage model for hyperelastic PUR adhesive

For the second application of the gradient enhanced damage model, the hyperelastic material model of [11] and [12] is applied to the PUR adhesive BETA FORCE 2850L. The damage theory of this material model consists of an isochoric and a volumetric part, based on the MOONEY-RIVLIN formulation of strain energy. This damage model has a high mesh sensitivity and was, therefore, extended by the gradient enhanced nonlocal damage model to regularise the mesh dependence of the material.

The regularisation is validated by a simple shear specimen, whereby the dimensions can be found in Fig. 8 d). The mesh dependence can be seen in the results of the calculation with different numbers of elements (Fig. 8 a). With the gradient enhanced damage model, proposed in this paper, the mesh dependence due to instability during strain softening is completely removed (Fig. 8 b). With this stability achieved in the calculation, it is possible to optimise the damage parameters in the damage model proposed by [11] using the experimental data from [12]. This optimisation is carried out in [18].

The results of the optimisation are depicted in Fig. 8 c). Before using this regularisation method, it was not possible to calculate the stress response during strain softening. The results correlate well with the test data for the two shear specimens, including different adhesive layer thicknesses.

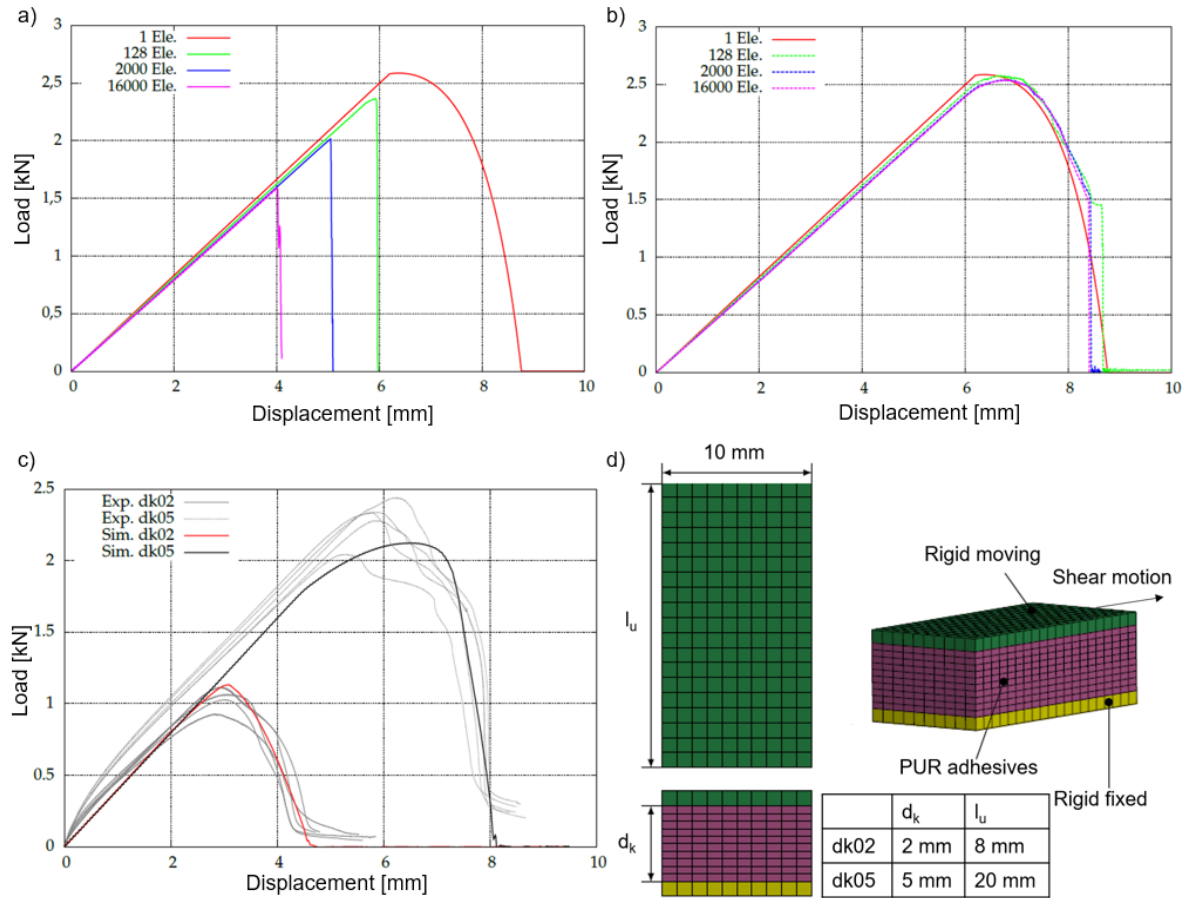


Fig.8: Simulation of a shear specimen using the material model for the PUR adhesive proposed in [11] a) Mesh study results of the shear specimen dk05 without regularisation b) the same mesh study with gradient enhanced damage c) results after optimisation of damage parameter compared to test data from [12] d) geometry of the shear specimen

6 Summary

At first, the problem of the pathological mesh sensitivity is outlined by simulations of a simple tensile bar with different mesh sizes. The modelling of the gradient enhanced damage approach is discussed, based on a TAYLOR series expansion of the integral nonlocal formulation. Thereby, the nonlocal damage variable is introduced, which replaces the local damage variable in continuum damage mechanics based material models. Since the resulting HELMHOLTZ type differential equation represents an analogous field problem to the heat equation, an efficient implementation into LS-DYNA® is explained by exploiting its thermo-mechanical coupled solver. Thereby, the nodal temperature is replaced by the nonlocal damage variable. The implementation is carried out on the basis of the mechanical user-material subroutine `umat` and the subroutine for the thermal user-material `thumat`. A successful verification of the implementation is presented for the tensile bar example, whereby the numerical solution, obtained by the gradient enhanced damage model, is compared to the outcome with the `*MAT_NONLOCAL` keyword in terms of stress-strain curves for different mesh sizes as well as the damage distribution prior to failure along the bar.

In order to demonstrate the simplicity of integrating the gradient enhancement for user defined material models, two existing continuum damage models are considered: a stress state dependent damage approach for ductile steels and a failure model for hyperelastic PUR adhesives. The

simulation results are compared to the according test data for various specimens, showing a good agreement within the region of softening material behaviour. Moreover, mesh insensitivity is demonstrated. In the case of the stress state dependent damage approach for ductile steels, the gradient enhanced approach is compared to the ***MAT_NONLOCAL** model in terms of the stress-strain curves and the elapsed simulation time. Although the model response is nearly identical for both nonlocal methods, a strong reduction of the simulation time in favour of the gradient enhanced damage method is revealed, compared to the ***MAT_NONLOCAL** option.

References

- [1] Drucker, D.C.: "A Definition of Stable Inelastic Material", *Journal of Applied Mechanics*, vol. 26, 1959, pp. 101–106.
- [2] Lemaitre, J.: "A Continuous Damage Mechanics Model for Ductile Fracture", *Journal of Engineering Materials and Technology*, vol. 107, 1985, pp. 83–89.
- [3] Azinpour, E., Ferreira, J. P. S., Parente, M. P. L., and Cesar de Sa, J.: "A simple and unified implementation of phase field and gradient damage models", *Advanced Modeling and Simulation in Engineering Sciences*, vol. 5, 2018.
- [4] Seupel, A., Hütter, G., and Kuna, M.: "An efficient FE-implementation of implicit gradient-enhanced damage models to simulate ductile failure", *Engineering Fracture Mechanics*, vol. 199, 2018, pp. 41–60.
- [5] Ostwald, R., Kuhl, E., and Menzel, A.: "On the implementation of finite deformation gradient-enhanced damage models", *Computational Mechanics*, vol. 64, 2019, pp. 847–877.
- [6] Pijaudier-Cabot, G. and Bazant, Z.: "Nonlocal Damage Theory", *Journal of Engineering Mechanics*, vol. 113, 1987, pp. 1512–1533.
- [7] Livermore Software Technology Corporation (LSTC): "LS-DYNA® Keyword User's Manual", Volume II - Material Models, LS-DYNA R11.0, Livermore, California, USA, 2018
- [8] Peerlings, R. H. J., de Borst, R., Brekelmans, W. A. M., and de Vree, J. H. P.: "Gradient enhanced damage for quasi-brittle materials", *International Journal for Numerical Methods in Engineering*, vol. 39, 1996, pp. 3391–3403.
- [9] De Borst, R., Pamin, J., Peerlings, R. H. J., and Sluys, L. J.: "On gradient-enhanced damage and plasticity models for failure in quasi-brittle and frictional materials", *Computational Mechanics*, vol. 17, 1995, pp. 130–141.
- [10] Rabotnov, Y. N.: "Creep Rupture", in: Hetényi M., Vincenti W.G. (eds) *Applied Mechanics*, International Union of Theoretical and Applied Mechanics, Springer, Berlin, Heidelberg, 1969, pp. 342-349.
- [11] Nelson, A.: "Modellierung und Finite-Elemente-Berechnung form- und stoffschlüssiger Fügeverbindungen", Bd. 1/2019. *Berichte des Instituts für Mechanik*. Kassel, Kassel University Press, <https://www.uni-kassel.de/ub/?id=39129&s=978-3-7376-0684-4>, 2019, pp. 96-178.
- [12] Nelson, A. and Matzenmiller, A.: "Numerische Modellierung und Kennwertermittlung für das Versagensverhalten von hyperelastischen Klebverbindungen", *Forschungsvereinigung Stahlanwendung e.V. (FOSTA)- Abschlussbericht zu P 1086*, 2017, pp. 123-130.
- [13] Nahrman, M. and Matzenmiller, A.: "Modelling of nonlocal damage and failure in ductile steel sheets under multiaxial loading", *International Journal of Solids and Structures*, vol. 232, 111166, 2021.
- [14] Nahrman, M. and Matzenmiller, A.: "Modelling stress-state dependent nonlocal damage and failure of ductile metals", *Proceedings in Applied Mathematics and Mechanics*, vol. 20, e202000054, 2021.
- [15] Nahrman, M. and Matzenmiller, A.: "Nonlocal damage modelling for finite element simulations of ductile steel sheets under multiaxial loading", *Proceedings in Applied Mathematics and Mechanics*, in print, 2021.
- [16] Mohr, D. and Marcadet S. J.: "Micromechanically-motivated phenomenological Hosford-Coulomb model for predicting ductile fracture initiation at low stress triaxialities", *International Journal of Solids and Structures*, vol. 67-68, 2015, pp. 40–55.
- [17] Trondl, A. and Klitschke, S. and Böhme, W. and Sun, D.-Z.: "Verformungs- und Versagensverhalten von Stählen für den Automobilbau unter crashartiger mehrachsiger Belastung", *FAT-Schriftenreihe 283*, *Forschungsvereinigung Automobiltechnik e.V.*, 2016.
- [18] Schmidt, H.: "Regularisierung durch Gradientenerweiterung für netzunabhängige FE-Simulationen von Montageklebverbindungen", *Masterthesis*, University of Kassel, Department of Mechanical Engineering, Institute of Mechanics, Kassel, 2019, pp. 66-70.